applied sciences

MDPI

Article

Single and Multivariate Statistics of Jet-Induced Pressure Fluctuations over an Infinite Plate

Stefano Meloni [1,*], Roberto Camussi [1], Alessandro Di Marco [1] and Matteo Mancinelli [2]

[1] Department of Engineering, University of RomaTre, 00185 Rome, Italy; roberto.camussi@uniroma3.it (R.C.); alessandro.dimarco@uniroma3.it (A.D.M.)

[2] Département Fluides, Thermique et Combustion, Institut Pprime—CNRS-Université de Poitiers-ENSMA, Chasseneuil-du-Poitou, 86000 Poitiers, France; matteo.mancinelli@univ-poitiers.fr

* Correspondence: stefano.meloni@uniroma3.it

Received: 27 May 2020; Accepted: 1 July 2020; Published: 2 July 2020

Abstract: Motivated by the problem of the installation effects of modern turbofan engines, we experimentally investigated the interaction between a compressible subsonic jet and a tangential flat plate. Measurements of wall pressure fluctuations were performed in a semi-anechoic environment addressing the effect of several governing parameters, such as the stream-wise and span-wise location, the jet Mach number and the radial distance of the plate surface from the jet axis. The statistical properties of the wall pressure signals were analyzed in terms of both power spectra and cross-correlations, with the latter providing the estimation of the phase speed. The analysis is also carried out in the time-frequency domain through the application of the wavelet transform to further characterize the dynamics of the wall pressure signatures.

Keywords: jet noise; wall pressure fluctuations; wavelet

1. Introduction

One of the most important topics of current research into aircraft engines concerns the reduction of noise and pollutant emissions. The strategy used by aircraft manufacturers to mitigate CO_2 release is to reduce the mass-flow rate passing in the engine's combustion chamber, thus exhausting from the primary nozzle. In order to keep the same level of thrust, the reduction of jet velocity must be compensated by increasing the mass-flow rate passing outside of the engine primary body. Given that the noise emissions from the engine jets are essentially proportional to the eighth power of the velocity according to Lighthill [1], the mass-flow increase in the secondary flow must be achieved by increasing the nozzle size rather than the exhausting jet velocity.

The ultra-high by-pass ratio (UHBPR) engine concept provides this solution, achieving a reduction of jet velocity and an increase of the fan/nacelle diameter. Design constraints in terms of ground clearance cause a more aggressive close-coupled architecture for the under-wing installation of the engine and thus a stronger jet-wing/flap interaction.

The interaction between the exhausting jet flow and the wing surface induces an increase of the radiated noise, thus jeopardizing the noise reduction due to the jet velocity decrease. On the other hand, the increasing size of the fan/nacelle diameter will lead to stronger jet–fuselage interactions as well, thus generating more severe concerns in terms of panel stress and vibrations. These vibrations underpin the transmission of interior noise in the fuselage, causing passenger annoyance, as well as the re-emission of vibration noise in the exterior aeroacoustic field. Aircraft and engine manufacturers are investing in research to mitigate these installation effects in the design of future under-wing engine configurations.

For the above-mentioned reasons, installation effects have been the subject of several works in the past and recent literature [2–5]. In this context, an important link between the wall pressure fluctuations and the far-field noise was addressed by Amiet [6], who developed a model to predict the far-field noise from the wall pressure fluctuations.

The effect of a surface on the emitted far-field noise was provided by[7], and the scattering effect of a tangential flat plate was also investigated by Cavalieri et al. [8] using a wavepacket noise-source model. The modification induced by a tangential flat plate on the jet aerodynamics was studied by [9,10] who outlined how the jet bent towards the surface when the mutual distance between the jet and the flat plate was of the order of the nozzle diameter. The tonal dynamics that occur when an isothermal turbulent jet interacts with a flat-surface edge were investigated through hydrodynamic and acoustic pressure measurements [11]. Studies on small-scale jet wing configurations were performed numerically [12] and experimentally [13].

The investigation of the wall pressure field induced by a jet over a surface located nearby seems to be the missing piece of this puzzling problem. This configuration has been studied in incompressible conditions by [14], laying the foundations for wall pressure fluctuation modeling by deriving scaling laws for pressure autospectra and coherence functions. The effects of the jet–plate distance on the cross and conditioned statistics between velocity and wall pressure fields were explored in [9]. More recently, the effect on the wall pressure statistics of different jet Mach numbers spanning the compressible subsonic regime was investigated in [15], whereas the effect of the jet Reynolds number was addressed by [16] (see also [17] for a general overview).

The objective of the present work is to explore, in a systematic fashion, the dependence of the jet–plate complex flow physics upon the main governing parameters, namely the jet Mach number M_j, the radial distance H of the flat plate from the nozzle axis and the spatial location of the pressure transducers on the surface in both the stream-wise (x) and span-wise (y) directions.

The pressure signals, measured by a pair of pressure transducers flush-mounted over the plate, are characterized in terms of single-point and two-point statistics in the time and frequency domains. The study is mainly devoted to a very aggressive jet–plate configuration, i.e., with the plate positioned at H/D = 0.75 from the nozzle axis. For such a small jet–plate distance, the jet plume heavily interacts with the plate, and a turbulent boundary layer (TBL)-like zone develops. A complete characterization of the wall pressure fluctuations in this region is carried out, and the results are compared with those obtained from a less aggressive jet–plate architecture, i.e., H/D = 2. Furthermore, a wavelet analysis is performed using the continuous wavelet transform (CWT) in order to provide a more complete characterization of the wall pressure signatures induced by the compressible jet over the flat plate.

The paper is organized as follows: Section 2 is devoted to the experimental set up and instrumentation description, the results are presented in Section 3 and conclusions are discussed in Section 4.

2. Experimental Setup

Experiments were carried out in the laboratory of fluid dynamics “G. Guj” of University Roma Tre. Measurements were performed in an acoustically treated chamber that measured 2 m × 4 m × 3 m. The characteristics of the semi-anechoic chamber have been amply described in previous papers (see, among many, [15,16,18]). A jet connected to a 2 m^3 air tank at 8 bar was installed in the semi-anechoic chamber. The connection was provided through a series of valves, and the duct was equipped with mesh screen and a honeycomb. An electronic pressure regulator was used for the remote control of the jet flow and maintained the nozzle pressure ratio to within 1% of the desired set point. Static pressure and temperature were continuously measured at the nozzle inlet. A J-type thermocouple was used to measure the air temperature inside the duct, whereas the static pressure was measured using properly calibrated ICSensor pressure transducers (50 p.s.i full scale). The determination of the pressure and temperature at the inlet section of the nozzle allowed us to determine analytically the jet Mach number M_j at the nozzle exhaust through isentropic relations.

A rigid flat plate was placed parallel to the nozzle axis with a traverse system that permitted the correct plate positioning with respect to the jet axis in the z direction. The plate was made of aluminum to obtain a stiffness comparable to the metal alloy of the aircraft external structures. The plate surface was pre-drilled with 200 taps whose spacings in the stream-wise and span-wise directions were equal to the jet diameter D, that is 12 mm. A picture of the experimental setup, previously reported in [16], is shown in Figure 1.

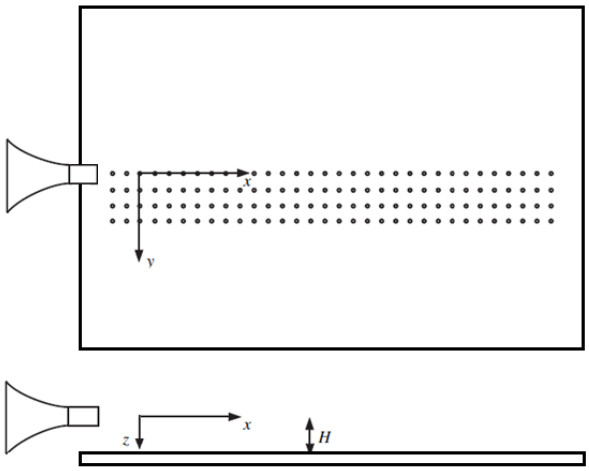

Figure 1. Experimental setup.

Wall pressure measurements were performed using two miniaturized pressure transducers (Kulite-Mic190M) whose size fit the pressure taps. These sensors have a sensitivity of 0.128 V/μbar, a dynamic range up to 194 dB and a frequency response up to 125 kHz, which corresponds to the mechanical resonant frequency. Pressure taps not involved in the measurement were covered to avoid spurious effects on the acquired signals. The pressure signals were acquired by a Yokogawa digital scope DL780E at a sampling frequency of 200 kHz with a cut-off filter set at 70 kHz and for a duration of 10 s. A more complete description of the experimental setup and instrumentation adopted can be found in [15,16].

Measurements were performed varying the radial position H of the flat plate from H/D = 0.75 to H/D = 2. The jet Mach number was varied from $M_j = 0.5$ up to $M_j = 0.9$. The pressure transducers were positioned for $1 \leq x/D \leq 25$ in the stream-wise direction and for $0 \leq y/D \leq 3$ in the span-wise direction. The nozzle diameter-based Reynolds numbers of these experiments were of the order of 10^5.

3. Results

3.1. Single-Point Statistics

The wall pressure statistics were characterized in the frequency domain through the power spectral density (PSD) evaluated with the Welch method [19] and presented as a function of the Strouhal number, defined as follows:

$$St = \frac{fD}{U_j}, \tag{1}$$

where f is the frequency and U_j is the nozzle exhaust velocity.

The axial evolution of the pressure spectra for two different plate positions (H/D = 0.75 and H/D = 2) is reported in Figure 2.

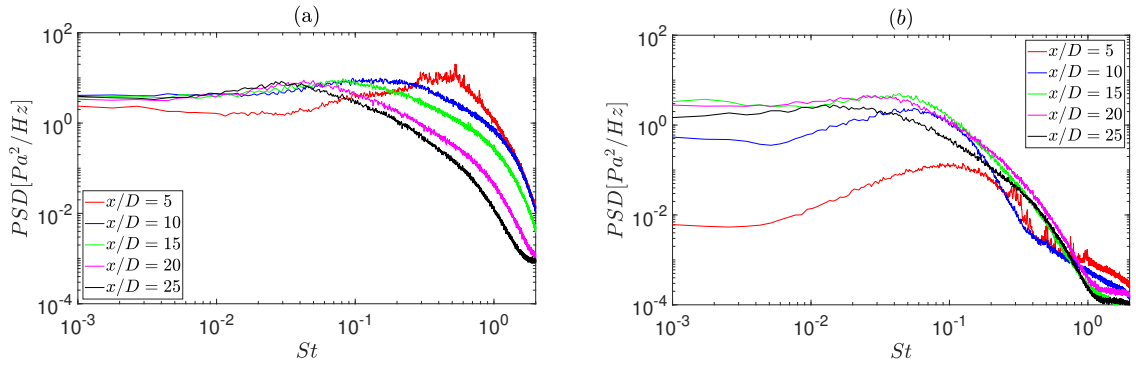

Figure 2. Axial evolution of the wall pressure autospectra at M_j = 0.5: (**a**) H/D = 0.75; (**b**) H/D = 2.

Different shapes are detected for H/D = 0.75 (Figure 2a) with respect to H/D = 2 (Figure 2b). This difference is ascribed to the different level of jet–surface interaction, which is related to the jet impact position over the flat plate. According to Grizzi and Camussi [18], the jet spreading angle is about 10°; therefore, in the case of H/D = 0.75, the jet is expected to impact the plate surface at about x/D ≈ 1.5. In agreement with [15,16], the jet impact point seems to be neither influenced by the different jet Mach numbers nor by the nozzle exhaust Reynolds numbers. Figure 2a shows peaks at x/D = 5 in the frequency range associated with the jet Kelvin–Helmholtz mode (i.e., between St = 0.2 and St = 0.5). At larger x/D, far downstream of the impact point, the shapes of the spectra becomes similar and the energy content decreases moving downstream. As reported in [15], the spectral shape follows the classical behavior expected for a fully developed TBL. Concerning the jet-plate configuration H/D = 2, the jet impacts the plate surface at about x/D ≈ 8.5 [15], thus inducing the development of a TBL-like zone further downstream with respect to the H/D = 0.75 configuration. The spectral behavior and the energy content vary accordingly with the more limited jet-surface interactions; three different interaction zones are presented in Table 1 [15,16,20]. Figure 2b shows that a significant energy bump is present at low frequencies for small axial distances (x/D ≤ 10) (i.e., free-jet zone), and this feature is the signature of the hydrodynamic pressure field, whereas the change in the spectral energy decay observed at high frequencies can be ascribed to the dominance of the acoustic pressure in the near region of the jet [21]. Furthermore, comparing x/D = 5 at H/D = 0.75, Figure 2a, with x/D = 10 at H/D = 2, Figure 2b, we point out that both positions were close to the jet impact point, although they showed a different spectral behavior influenced by the jet flow conditions. Indeed, we observe, at x/D = 5, a peak related to the Kelvin–Helmholtz roll-up, whereas at x/D = 10, a bump can be observed at lower St numbers due to the larger-scale turbulent structures generated by the jet development.

Table 1. Jet-plate interaction zones. TBL: turbulent boundary layer.

H/D	Free Jet Zone	Impact Zone	TBL-Like Zone
0.75	Not appreciable	1D-7D	7D-25D
2	1D-10D	10D-20D	20D-25D

The effect of the jet Mach number at H/D = 0.75 is reported in Figure 3a,b. It is shown that, for a fixed x/D, the spectral shape is weakly affected by M_j , in agreement with the results presented in our previous studies [15] where this behavior was observed for larger H/D vales.

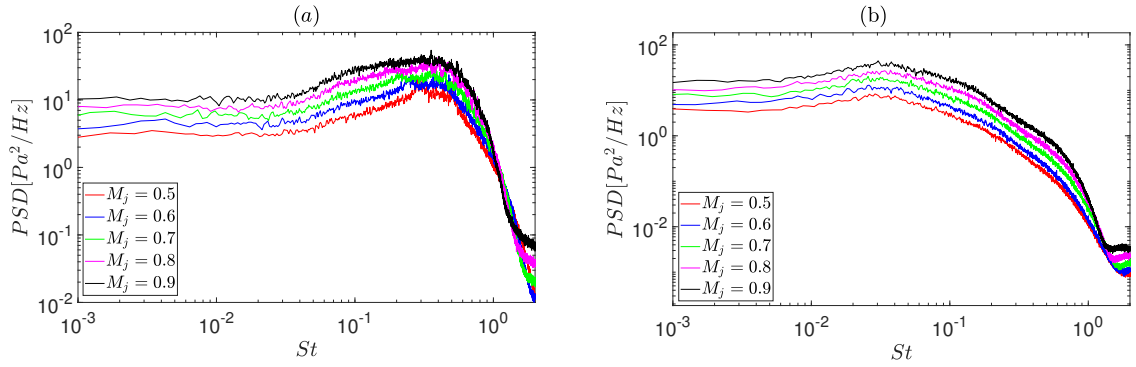

Figure 3. Mach number effect on the pressure autospectra for the jet–plate radial distance H/D = 0.75: (**a**) x/D = 5; (**b**) x/D = 25.

The wall pressure fluctuations were investigated in the span-wise direction as well, and results for two different stream-wise positions—i.e., x/D = 5 and x/D = 25—are reported in Figure 4. We note that both spectral energy and shape are affected by the different transverse position considered at x/D = 5 (see Figure 4a). Specifically, the energy content significantly decreases as the span-wise distance increases, and this behavior could be likely ascribed to the lower flow–surface interaction far away from the core of the jet. This interpretation is further supported by the results reported in Figure 4b, where the span-wise evolution is reported for a much larger stream-wise position; i.e., x/D = 25. We note that the differences in spectral shape among all the transverse positions observed for x/D = 5 disappear here, and the amplitude discrepancy is significantly reduced. This behavior is likely ascribed to the jet development far away from the nozzle exhaust, which induces a much wider footprint over the flat plate.

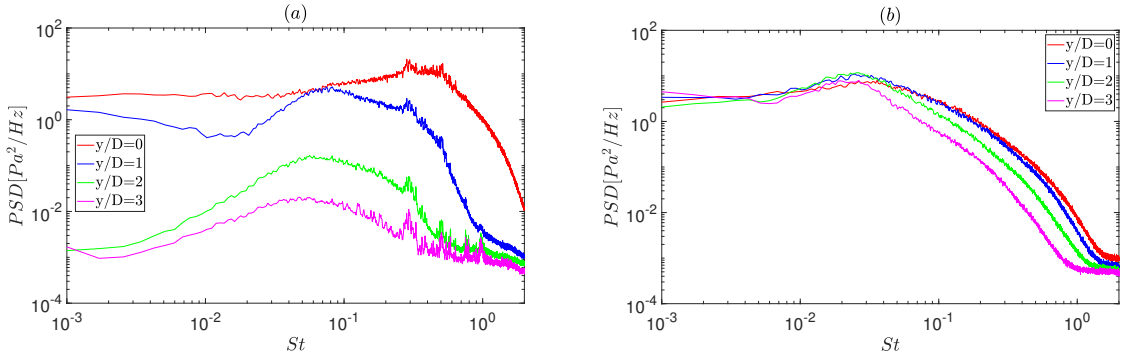

Figure 4. Span-wise evolution of the pressure autospectra for the jet–plate distance H/D = 0.75 and the jet Mach number M_j = 0.5: (**a**) x/D = 5; (**b**) x/D = 25.

3.2. Two-Point Statistics

The two-point statistics of the wall pressure fluctuations were characterized in the time domain in terms of the cross-correlation computed between two contiguous pressure transducers in both the stream-wise and span-wise directions. The cross-correlation function is defined as follows:

$$R_{pp} =< p(x,t), p(x+\xi, y+\eta, t+\tau) > \quad (2)$$

where ξ and η are the stream-wise and span-wise separations, respectively (in the present study, $\xi = \eta = 1D$), τ is the time lag and the symbol $<>$ denotes the ensemble average. The cross-correlation is normalized by dividing by the product of the standard deviations of the two pressure signals, providing the non-dimensional cross-correlation coefficient.

The axial evolution of the cross-correlation coefficient at plate radial distances of H/D = 0.75 and H/D = 2 is reported in Figure 5. The oscillatory pseudo-periodic trend observed at the axial

distances x/D = 5 and x/D = 6, is probably related to the jet hydrodynamic field (i.e., Kelvin–Helmholtz instability). At any rate, further analyses are required to better clarify this issue.

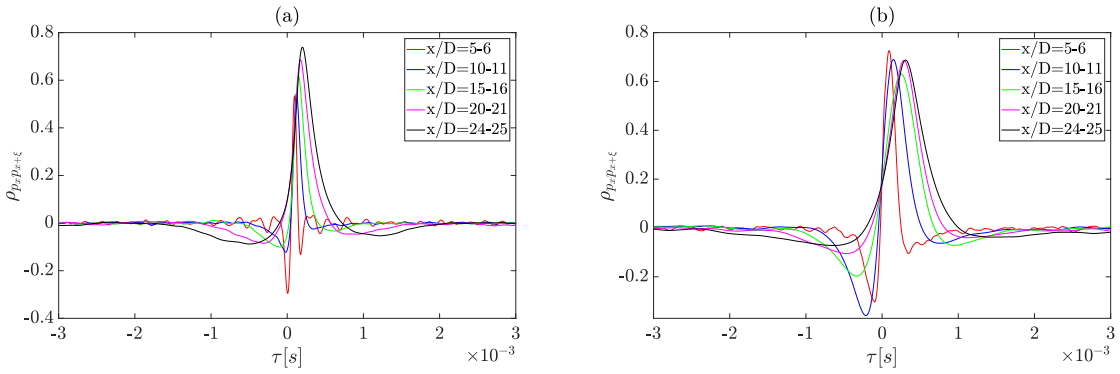

Figure 5. Axial evolution of the wall pressure cross-correlation coefficient at M_j = 0.5: (**a**) H/D = 0.75; (**b**) H/D = 2.

This effect is more evident at H/D = 0.75, because of the vicinity of the pressure transducers to the jet plume. For increasing axial distances, the negative bump observed for a small x/D progressively disappears and the time scale of the cross-correlations increases due to the development of large-scale structures in the jet plume. Comparing Figure 5a against Figure 5b, we note that a reduction of the flat plate radial position (H) induces a narrowing of the cross correlations. This is due to the breakup of the large-scale turbulent structures as the plate approaches the jet. In both configurations, the time delay of the cross-correlation peak increases for larger x/D, thus inducing a reduction of the phase speed of the associated flow structures. This effect is more perceptible at H/D = 0.75.

The effect of the jet Mach number on the cross-correlation coefficient is analyzed at x/D = 5 and x/D = 25 and reported in Figure 6a,b, respectively. Figure 6a shows that the oscillatory trend detected at x/D = 5 seems to be slightly reduced with increasing Mach numbers. We observe a reduction in the time delay associated with the first peak for increasing jet Mach numbers, thus revealing a dependence of phase speed upon the jet velocity—an effect that will be discussed in the next section. As reported in Meloni et al. [15], a similar behavior was observed at H/D = 2.

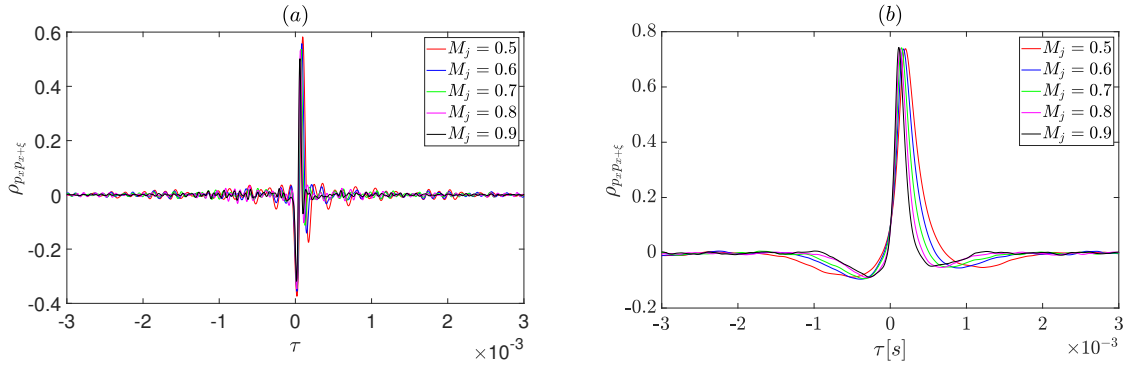

Figure 6. Mach effect on the wall pressure cross-correlation coefficient for the jet–plate distance H/D = 0.75: (**a**) x/D = 5; (**b**) x/D = 25.

Cross-correlations were evaluated also in the span-wise direction at two different axial locations x/D = 5 and x/D = 25, reported in Figure 7a,b, respectively. We observe an oscillatory trend that is slightly influenced by the different span-wise location in Figure 7a. Figure 7b shows an increase of the cross-correlation peak amplitude for increasing y/D—a trend that can be ascribed to the reduction of the turbulence level of the jet and hence the randomness of the associated time signal.

Furthermore, the time delay of the cross-correlation peak is close to zero and remains about constant in both Figure 7a,b, confirming that the convection effect is not relevant in the span-wise direction.

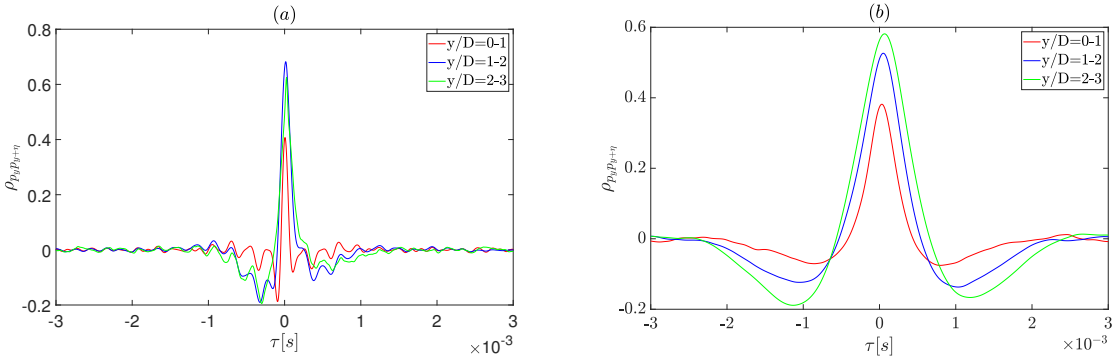

Figure 7. Span-wise evolution of the wall pressure cross-correlation coefficient for the jet-plate distance H/D = 0.75 and jet Mach number M_j = 0.5: (**a**) x/D = 5; (**b**) x/D = 25.

3.3. Wall-Pressure Phase Speed

The phase speed was evaluated from the time delay of the first cross-correlation peak by using the following equation:

$$U_{ph} = \frac{\xi}{\tau}, \tag{3}$$

where ξ is the distance between two consecutive pressure transducers and τ is the time delay of the first cross-correlation peak.

The phase speed normalized with respect to the nozzle exhaust velocity is reported in Figure 8. In agreement with the results presented in [15], the evolution of the phase speed is not influenced by the jet Mach number (Figure 8a), whereas Figure 8b shows that the plate radial position has a significant effect on the phase speed. When H/D is small, the phase speed decreases for a larger x/D due to the development of larger-scale turbulent structures as well as the reduction of the mean jet velocity. On the other hand, at larger H/D values, the propagation of acoustic waves at a velocity larger than the speed of sound is related to a motion of the acoustic wave front that is not parallel to the plate surface.

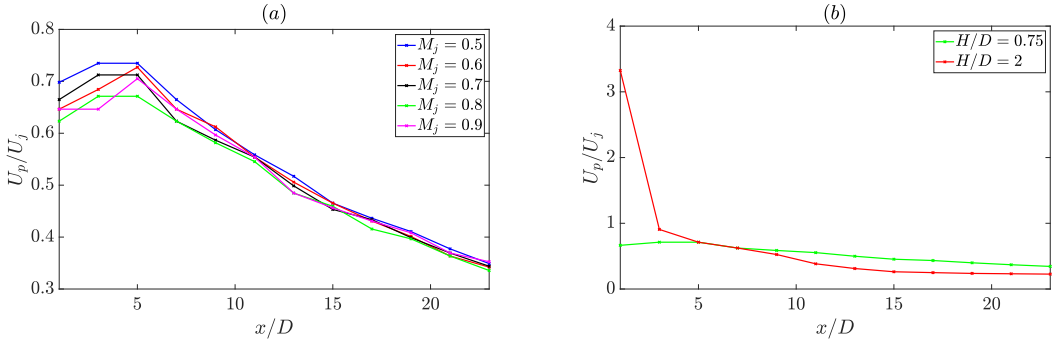

Figure 8. Wall pressure phase speed trends: (**a**) Mach effect at H/D = 0.75; (**b**) H/D comparison at M_j = 0.7.

3.4. Wavelet Analysis

The wavelet transform is used to highlight and identify intermittent events induced by the interaction between the compressible jet flow and the flat plate in the time–frequency domains. The analysis is performed using the continuous wavelet transform (CWT), consisting of the projection

of the pressure signal over a basis of compact-support functions obtained by the translation and dilation of a so-called mother wavelet function. The definition, according to [9,22], is reported as follows:

$$w(s,t) = C_{\psi}^{\frac{-1}{2}} s^{\frac{-1}{2}} \int_{-\infty}^{\infty} p(\tau)\psi^*\left(\frac{t-\tau}{s}\right), \quad (4)$$

where s is the wavelet scale , τ is a time shift, $C_{\psi}^{\frac{-1}{2}}$ is a constant that takes into account the mean value of $\psi(t)$ and $\psi^*\left(\frac{t-\tau}{s}\right)$ is the complex conjugate of the dilated and translated mother wavelet $\psi(t)$. The *bump* kernel is chosen as the mother wavelet; its analytic description is reported in [22,23].

Examples of wavelet scalograms, normalized by the maximum amplitude of the wavelet coefficients as a function of time and Strouhal, are reported in Figure 9 for different stream-wise locations, radial positions of the flat plate and jet Mach numbers. For the sake of conciseness, we only report the scalogram evolution for 0.1 s of time acquisition, which corresponds to about 10^3 characteristic flow times, thus ensuring the statistical representativeness of the results reported. We note that for a large jet–plate distance—that is, H/D = 2—the most energetic pressure events are located for a St number range lower than that associated with H/D = 0.75 (see the comparison between Figure 9a–d). This feature could be likely ascribed to the excitation of flow structures of a smaller scale as the plate approaches the jet, in agreement with the results shown above (see Figures 2a, 5a and 6a). We then underline that the effect of the jet Mach number on the appearance of the energetic wall-pressure events seems not to be significant (see the comparison between Figure 9a,c and Figure 9b,d). We finally note that, as expected, the distribution of energetic pressure events moves to a lower St for large x/D as a consequence of the flow development and the generation of large-scale flow structures for large stream-wise positions. This fits with the results presented in Figure 2a,b.

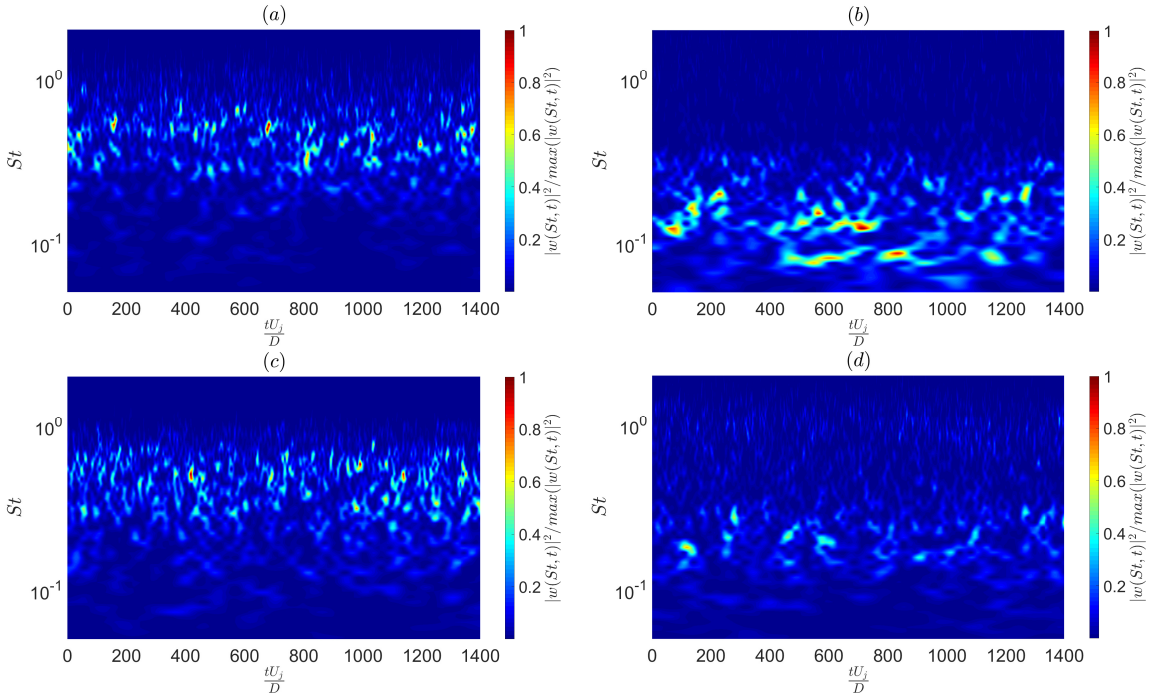

Figure 9. *Cont.*

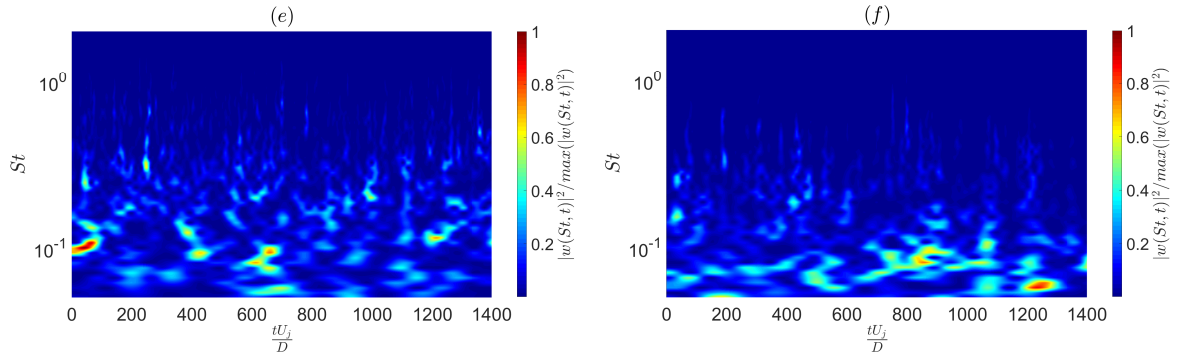

Figure 9. Wavelet scalograms—on the left, H/D = 0.75, on the right, H/D = 2—for: (**a**) x/D = 5 and M_j = 0.5; (**b**) x/D = 5 and M_j = 0.5; (**c**) x/D = 5 and M_j=0.9; (**d**) x/D = 5 and M_j=0.9; (**e**) x/D = 25 and M_j = 0.5; (**f**) x/D = 25 and M_j = 0.5.

4. Conclusions

The wall pressure fluctuations induced by a compressible jet over a tangential flat plate were experimentally investigated in the stream-wise and span-wise directions at different jet Mach numbers and radial positions of the flat plate. The pressure field over the plate was measured using two flush-mounted pressure transducers.

A spectral characterization was performed to characterize the wall-pressure energy content in the frequency domain. We showed that the interaction of the jet with the plate induces the development of TBL-like dynamics for the close-coupled configuration that modify both the spectral shape and energy content. The increase of the jet Mach numbers induces an increase of the spectra amplitudes without modifying their shape. Finally, the important influence of the jet development on the span-wise wall pressure spectra has been determined.

The analysis in the time domain was performed by computing the cross-correlation. The time delay and the shape of the cross-correlations are influenced by the position of the jet impact point as well as by the jet Mach number. Indeed, the development of a TBL-like zone over the plate leads to narrower cross-correlations, highlighting the breakup of jet turbulent structures due to the presence of the rigid plate. The wall pressure phase speed computed from the cross-correlation is weakly influenced by the Mach number but strongly dependent on the plate radial position in the region close to the jet exit. Moreover, as expected, irrelevant convection effects are detected in the span-wise direction.

A wavelet analysis was finally performed. The scalogram showed significant differences in terms of the excitation of flow scales between small and large jet–plate distances for stream-wise positions close to the nozzle exhaust. Conversely, at a large x/D, the different radial positions of the flat plate slightly affected the scalogram dynamics. No significant jet Mach number effects on the wavelet scalogram were observed for both jet–plate distances.

Author Contributions: Measurements, S.M.; Data analysis, S.M.; writing—original draft preparation, S.M., R.C., A.D.M., M.M.; writing—review and editing, S.M., R.C., A.D.M., M.M.; All authors have read and agreed to the published version of the manuscript.

Funding: This research received no external funding.

Conflicts of Interest: The authors declare no conflict of interest.

References

1. Lighthill, M.J. On sound generated aerodynamically. I. General theory. *Proc. R. Soc. Lond. A* **1952**, *211*, 564–587.
2. Head, M.; Fisher, R. Jet/surface interaction noise - Analysis of farfield low frequency augmentations of jet noise due to the presence of a solid shield. In Proceedings of the 3rd Aeroacoustics conference, Palo Alto, CA, USA, 20–23 July 1976. [CrossRef]

3. Lyu, B.; Dowling, A.P. An experimental study of the effects of lobed nozzles on installed jet noise. *Exp. Fluids* **2019**, *60*, 176. [CrossRef]
4. Lawrence, J.; Azarpeyvand, M.; Self, R.H. Interaction between a Flat Plate and a Circular Subsonic Jet. In Proceedings of the 17th AIAA/CEAS Aeroacoustics Conference (32nd AIAA Aeroacoustics Conference), Portland, OR, USA, 5–8 June 2011. [CrossRef]
5. Huber, J.; Drochony, G.; Pintado-Peno, A.; Cléro, F.; Bodard, G. Large-Scale Jet Noise Testing, Reduction and Methods Validation "EXEJET": 1. Project Overview and Focus on Installation. In Proceedings of the 20th AIAA/CEAS Aeroacoustics Conference, AIAA AVIATION Forum, AIAA 2014-3032, Atlanta, GA, USA, 16–20 June 2014. [CrossRef]
6. Amiet, R.K. Noise due to turbulent flow past a trailing edge. *J. Sound Vib.* **1976**, *46*, 387–393. [CrossRef]
7. Papamoschou, D.; Mayorlal, S. Experiments on shielding of jet noise by airframe surfaces. In Proceedings of the 15th AIAA/CEAS Aeroacoustics Conference (30th AIAA Aeroacoustics Conference), Miami, FL, USA, 11–13 May 2009; AIAA Paper 2009 2009-3326. [CrossRef]
8. Cavalieri, A.V.G.; Jordan, P.; Wolf, W.R.; Gervais, Y. Scattering of wavepackets by a flat plate in the vicinity of a turbulent jet. *J. Sound Vib.* **2014**, *333*, 6516–6531. [CrossRef]
9. Mancinelli, M.; Di Marco, A.; Camussi, R. Multivariate and conditioned statistics of velocity and wall pressure fluctuations induced by a jet interacting with a flat plate. *J. Fluid Mech.* **2017**, *823*, 134–165. . [CrossRef]
10. Proença, A.; Lawrence, J.L.T.; Self, R.H. Experimental study on the aerodynamics of a high subsonic jet interacting with a flat plate. In Proceedings of the 23rd ABCM International Congress of Mechanical Engineering, Rio de Janeiro, Brazil, 6–11 December 2015.
11. Jordan, P.; Jaunet, V.; Towne, A.; Cavalieri, A.; Colonius, T.; Schmidt, O.; Agarwal, A. Jet–flap interaction tones. *J. Fluid Mech.* **2018**, *853*, 333–358. [CrossRef]
12. Tyacke, J.C.; Wang, Z.N.; Tucker, P.G. LES-RANS of Installed Ultra-High-Bypass-Ratio Coaxial Jet Aeroacoustics with Flight Stream. *AIAA J.* **2019**, *57*, 1215–1236. doi:10.2514/1.j057057. [CrossRef]
13. Meloni, S.; Mancinelli, M.; Camussi, R.; Huber, J. Wall-Pressure Fluctuations Induced by a Compressible Jet in Installed Configuration. *AIAA J.* **2020**. [CrossRef]
14. Di Marco, A.; Mancinelli, M.; Camussi, R. Pressure and velocity measurements of an incompressible moderate Reynolds number Jet interaction with a tangential flat plate. *J. Fluid Mech.* **2015**, *770*, 247–272. [CrossRef]
15. Meloni, S.; Di Marco, A.; Mancinelli, M.; Camussi, R. Wall-pressure fluctuations induced by a compressible jet flow over a flat plate at different Mach numbers. *Exp. Fluids* **2019**, *60*, 48. [CrossRef]
16. Meloni, S.; Di Marco, A.; Mancinelli, M.; Camussi, R. Experimental investigation of jet induced wall pressure fluctuations over a tangential flat plate at two Reynolds numbers. *Sci. Rep.* **2020**, *10*, 9140. [CrossRef] [PubMed]
17. Meloni, S.; Di Marco, A.; Mancinelli, M.; Camussi, R. Parametric characterization of wall pressure fluctuations induced by a compressible jet flow interacting with a flat plate. In Proceedings of the 25th AIAA/CEAS Aeroacoustics Conference, Delft, The Netherlands, 20–23 May 2019. [CrossRef]
18. Grizzi, S.; Camussi, R. Wavelet analysis of near-field pressure fluctuations generated by a subsonic jet. *J. Fluid Mech.* **2012**, *698*, 93–124. [CrossRef]
19. Welch, P. The use of fast Fourier transform for the estimation of power spectra: A method based on time averaging over short, modified periodograms. *IEEE Trans. Audio Electroacoust.* **1967**, *15*, 70–73. [CrossRef]
20. Mancinelli, M.; Camussi, R. An experimental investigation of the wall pressure field induced by a low and moderate Mach numbers jet on a tangential flat plate. In Proceedings of the 2018 AIAA/CEAS Aeroacoustics Conference, AIAA AVIATION Forum, AIAA 2018-3616, Atlanta, GA, USA, 25–29 June 2018.
21. George, W.; Beuther, P.; Arndt, R. Pressure spectra in turbulent free shear flows. *J. Fluid Mech.* **1984**, *148*, 155–191. [CrossRef]

22. Meloni, S.; Lawrence, J.; Proença, A.; Self, R.; Camussi, R. Wall pressure fluctuations induced by a single stream jet over a semi-finite plate. *Int. J. Aeroacoust.* **2020**. [CrossRef]
23. Mancinelli, M.T.; Jaunet, V.; Jordan, P.; Towne, A. Screech-tone prediction using upstream-travelling jet modes. *Exp. Fluids* **2019**, *60*, 22. [CrossRef]